Check for updates

Differentially expressed genes in head kidney of *Pelteobagrus fulvidraco* following *Vibrio cholerae* challenge

Sen-Hao Jiang[1,2], Lin-Xin Wu[1], Yu-Ting Cai[1], Rui-Ting Ma[3], Hua-Bin Zhang[1], Dai-Zhen Zhang[1], Bo-Ping Tang[1]*, Qiu-Ning Liu[1]* and Li-Shang Dai[2]*

[1]Jiangsu Key Laboratory for Bioresources of Saline Soils, Jiangsu Synthetic Innovation Center for Coastal Bio-agriculture, Jiangsu Provincial Key Laboratory of Coastal Wetland Bioresources and Environmental Protection, School of Wetlands, Yancheng Teachers University, Yancheng, China, [2]School of Pharmaceutical Sciences, Wenzhou Medical University, Wenzhou, China, [3]School of Urban and Planning, Yancheng Teachers University, Yancheng, China

The yellow catfish (*Pelteobagrus fulvidraco*) is a freshwater fish with high economic value in eastern China. Nevertheless, pathogens causing bacterial diseases in *P. fulvidraco* have brought about huge economic loss and high mortality in artificial aquaculture. For disease control, it is critical to further understand the immune system of yellow catfish and immune-related genes with which they respond to pathogenic infections. In this study, high-throughput sequencing methods were used to analyze the transcriptomic spectrum of the head kidney from *P. fulvidraco* challenged by *Vibrio cholera*. A total of 45,544 unique transcript fragments (unigenes) were acquired after assembly and annotation, with an average length of 1,373 bp. Additionally, 674 differentially expressed genes (DEGs) were identified after stimulation with *V. cholerae*, 353 and 321 genes were identified as remarkably up- or downregulated, respectively. To further study the immune-related DEGs, we performed KEGG enrichment and GO enrichment. The results showed gene regulation of response to stimulus, immune response, immune system progress, response to external stimuli and cellular response to stimuli. Analysis of KEGG enrichment is important to identify chief immune related pathways. Real-time quantitative reverse transcription-PCR (qRT-PCR) results indicated 10 immune response genes that were found to be upregulated compared to a control group after 6 h of *V. cholerae* challenging. In summary, the results of our study are helpful to determine the defense mechanisms and immune system responses of yellow catfish in reaction to bacterial challenges.

KEYWORDS

pelteobagrus fulvidraco, transcriptome, *Vibrio cholerae*, differential expressed genes, immune response

Introduction

Yellow catfish has been extensively farmed and is an economically significant freshwater species in China, South Korea, Japan, and South Asia (1–3). The popularity of this species has rapidly increased recently because of its tender flesh, few bones, and good taste (4, 5). Consequently, the market demand for yellow catfish in China is very large, and its price very high. In recent years, the rapid growth of *P. fulvidraco* aquaculture has caused a huge decline in their population due to microbial disease, including viruses, parasites, and bacteria, which has brought about huge economic losses (6). However, little is known about the molecular mechanisms relevant to immunity. Recently, *P. fulvidraco* has been employed as an experimental model fish to investigate breeding techniques, development, lipid metabolism, immunology and toxicology (7–11). *Vibrio cholerae*, is an aquatic, gram-negative bacterium, which is responsible for pandemics of cholera disease worldwide (12). To decrease the danger of aquaculture, understanding molecular defense mechanisms of yellow catfish against microbial diseases is indispensable to establish reasonable control measures.

High-throughput RNA-sequencing (RNA-Seq) is a low-cost technique with high sensitivity, wide genome coverage, and unbiased quantification of transcript expression which is a relatively new technique that allows transcriptome analysis (13). Transcriptome analysis is widely used in genome research and functional gene identification, particularly for understanding hereditary responses to pathogens (14). In addition, transcriptome research has been increasingly applied to many fields of research including physiology, ecology, evolution and genetics, and has been critical for gene expression analysis, genetic marker mining, and gene discovery in many species (15). Recently, a variety of comparative transcriptomic studies focusing on fish immune responses after exposure to microbial pathogens were performed, such as in crucian carp (16), rainbow trout (17), half-smooth tongue sole (18), blunt snout bream (19), tilapia (20), soiny mullet (21), and miiuy croaker (22).

In this study, based on the head kidney of *P. fulvidraco* from PBS-control and *V. cholerae* infected groups, we established two transcriptome sequence libraries. Similar to the mammalian adrenal gland, the head kidney is an important endocrine and haematopoietic-lymphoid organ which is unique for teleost fish and participates in innate immune responses to pathogen infections (23). By comparison among the libraries, differentially expressed genes (DEGs) were recognized. Through gene ontology (GO) enrichment and Kyoto Encyclopedia of Genes and Genomes (KEGG) enrichment, these DEGs were enriched and the immune-related DEGs were identified that maybe provide insights into the potential molecular immune mechanisms of *P. fulvidraco*.

Materials and methods

Experimental fish models

Yellow catfish were collected from the aquatic market, Yancheng, Jiangsu Province, China, in October 2020 and were acclimatized in tanks at 24°C for two weeks before the experiment commenced. The fish were then divided into two groups, each containing three fish: a control group and the *V. cholerae* group. The control group was injected with 100 μL PBS whilst the *V. cholerae* group were injected with the same dose of bacterial suspension that had a final concentration of 1×10^7 CFU/mL and were treated as the experimental group. The head kidneys were gathered 6 h after injection and stored at -80°C.

RNA extraction, library construction and Illumina sequencing

Library constructions were performed at the Novogene Experimental Department (Beijing, China). RNA -easy isolation reagent (Vazyme, China) was used to extract the total RNA content of the head kidney. RNA degradation, purity, and contamination were measured by 1% agarose gels, NanoPhotometer® spectrophotometer (IMPLEN, CA, USA), and Qubit® 2.0 Fluorometer. RNA integrity was evaluated by the Agilent Bioanalyzer 2100 system (Agilent Technologies, CA, USA). We made use of the NEBNext® Ultra™ RNA Library Prep Kit for Illumina® (NEB, USA) to generate sequencing libraries. Random hexamers primers and M-MuLV were utilized for first strand cDNA synthesis, using DNA Polymerase I and RNase H for synthesis of the second strand. Purification of the PCR products involved the following steps: purification, adapter addition, and cDNA fragment selection, and PCR by universal PCR primers and Index (X) Primers. Finally, the insert size of the library from the libraries was sequenced using an Illumina HiSeq platform at Novogene.

Sequencing data processing and assembly

Through in-house Perl scripts, we first processed raw reads of FASTA formatted sequences. In this procedure, by deleting reads such as those generated by adapters, clean reads were obtained, consisting of poly-N and low-quality reads from raw reads. Then, to obtain the reference sequence for subsequent analysis, we concatenated the clean reads. By using Trinity software, the compilation of *de novo* transcriptome data was executed by three independent components: Butterfly, Chrysalis, and Inchworm (24). Finally, the longissimus transcript of every gene was named unigenes. Meanwhile, based on clean reads with

high quality, Q-value 20, Q-value 30, GC-content, and sequence duplication level of the clean reads were calculated.

Unigenes annotation and functional enrichment

Unigenes were annotated by comparison to seven databases and processed by BLAST. The databases included: NT (NCBI non-redundant nucleotide sequences, e-value=1e-5), NR (NCBI non-redundant protein database, e-value=1e-5), Eukaryotic Orthologous Groups (KOG/COG) (http://www.ncbi.nlm.nih.gov/COG/, e-value=1e-3), Pfam (http://pfam.sanger.ac.uk/, e-value=0.01), GO (http://www.geneontology.org/, e-value=1e-6) (25), KEGG (http://www.genome.jp/kegg, e-value=1e-10), and Swiss-prot (http://www.ebi.ac.uk/uniprot/, e-value=1e-5). GO annotation of unigenes was derived from NR annotation by the Blast2GO program, and WEGO software was used to perform GO functional classification (26). Pathway assignments were executed using the KEGG database (27).

Identification of DEGs

To estimate DEGs between two datasets, expression levels of unigenes were calculated using the FPKM method, the universal method for detecting gene expression (28). For the sake of calculating the expression profiles between PBS and *V. cholerae*-injected head kidney tissues, we made use of RSEM software to map the clean data (29). We obtained a read count for each gene from the mapping results. Before DEGs analysis, all read counts were normalized using edgeR (30). DEGs analysis of two libraries was carried out using the DEGseq R package (31). The *p*-value was adjusted according to the q-value. Q-value<0.005 and |log$_2$(fold change)|>1 were assigned as differential expression genes. Then DEGs were subjected to KEGG pathway analysis and GO functional enrichment analysis. By Wallenius noncentral hypergeometric distribution, we employed GOseqR to implement GO enrichment analysis of DEGs, which can be adjusted for gene length bias in DEGs (32). KOBAS software was used to test the statistical enrichment of DEGs in the KEGG pathway (33).

qRT-PCR of candidate gene expression

qRT-PCR was employed to check the expression level of the 10 candidate DEGs. Following the manufacturer's instructions, MightyScript Plus First Strand cDNA Synthesis Master Mix (gDNA digester) (Sangon, China) was used to produce synthesized cDNA that acted as a template for qRT-PCR. Primer premier 5.0 software was then used to design candidate DEGs primers with reference to the cDNA sequence. The β-actin gene from *P. fulvidraco* was used as an internal reference. The sequences of PCR primers are shown in Table 1. By using Mastercycler ep realplex (Eppendorf, Germany) with the AceQ Universal SYBR qPCR Master Mix (Vazyme, China), qRT-PCR was performed in 20 μl reaction mixtures consisting of 10 μl 2×SYBR Green mix, 1 μl cDNA, 7 μl RNase-free H$_2$O, and 1 μl forward and reverse primers. The steps of PCR were as follows: 20 s at 95℃, followed by 40 cycles of 15 s at 95℃ and 15 s at 55℃, then at 72℃ 20 s and 60℃ for 1 min. Each independent experiment was performed in triplicate and determined the relative expression levels of the genes which was calculated with the $2^{-\triangle\triangle CT}$ comparative threshold cycle (Ct) method (34).

TABLE 1 Primers used for qRT-PCR in this paper.

Primer name	Forward Primer (5′-3′)	Reverse Primer (5′-3′)	Purpose
cadherin-5	GTGAACGCAACCAACGTCTT	CCCACAGGCTCATCCTCATT	qRT-PCR
CC chemokine SCYA101	GCTGCAAGAAGACGAGTTGA	CCATCGCTCTAGCCAGTAAG	qRT-PCR
calumenin	AGAGTGGGTGAAGACAGAGCG	TTCGTACAGCAGGTGTTTGG	qRT-PCR
C-type lectin	TATTCTGGTCGCTGCTACTTG	AGCCCTTATCTGCTGATATTCA	qRT-PCR
interleukin-13 receptor	TGGGTCTTCTGAGGTGGGATA	GTTGCTTGTTGCCAGTGAGG	qRT-PCR
Integrin	GAACTCGCTCAGGGAGGATT	ATGCGTTGATGAATGAAGTGTTT	qRT-PCR
LAMP 1	CAGCACTTTCACCCTCAACA	AACAACCCTGGAAACAAACAT	qRT-PCR
Mucin-2	CACCATATTCAGACCGTCAT	CAGTTCATCGTACAGCACCT	qRT-PCR
Natterin	TGTAAGACTCAGCACCACCC	GAGAATCACCTTCCCAAACC	qRT-PCR
Nramp	TCGCCTTCAACCTGCTGTCT	CAATCCCAACTGCCTGCTCT	qRT-PCR
β-actin	GCACAGTAAAGGCGTTGTGA	ACATCTGCTGGAAGGTGGAC	qRT-PCR

Statistical analysis

Statistical analysis was used to examine the differences of mRNA expression levels and performed using the statistical software SPSS 17.0 and $p<0.05$ results were considered significant. All quantitative data were expressed as means ± SD at least three independent experiments.

Results and discussion

Sequencing and *de novo* assembly

To acquire the transcriptomic analysis data of the *P. fulvidraco* head kidney following injection of *V. cholerae*, we employed Illumina HiSeq sequencing platform to construct two libraries, and the results are summarized in Table 2 (13). Approximately, 53,492,522 and 47,733,280 clean reads were noted from the yellow catfish head kidney in *V. cholerae* challenged and PBS-challenged fish. Each sample had a quality score over 96% and 91% with Q-value 20 and Q-value 30, respectively, and that the GC content of each library was approximately equal (44%). We spliced all the clean data into 135,097 transcripts (total length of 226,790,028) with a mean length of 1,697, N50 length of 2,854, and N90 length of 677 (Table 3). We further assembled 45,544 unigenes (total length of 62,537,256) with an average length of 1,373, N50 length of 1,439, and N90 length of 536. These results show that the transcriptome data were reliable, and the sequence data were high-quality.

After assembly, the length of unigenes extended from 301 bp to 19,263 bp with a length of 1,373 bp on average. The length of assembled unigenes indicated that 12,679 of unigenes extended from 300 bp to 500 bp, 15,482 of unigenes extended from 500 bp to 1000 bp, 7,917 of unigenes extended from 1,000 bp to 2,000 bp, and 9,466 of unigenes were more than 2,000 bp. In addition, the length of transcripts showed that 30,391 transcripts ranged from 500 bp to 1,000 bp, 36,228 of transcripts ranged from 300 bp to 500 bp, 28,521 of transcripts ranged from 1,000 bp to 2,000 bp, and 39,957 of transcripts exceeded 2,000 bp (Figure 1).

Annotation of assembled unigenes

To gain a comprehensive view of gene function information, 45,544 unigenes were annotated by seven databases including NR, NT, Swiss-Port, KOG, PFAM, GO, and KO (35). Of these unigenes, 29,004 unigenes (63.68%) were annotated in one database at least, and 5,544 unigenes (12.17%) were constructed in all databases. The number of unigenes that may be annotated in diverse databases was 24,521 in NR (53.84%), 20,034 in NT (43.98%), 11,300 in KO (24.81%), 16,032 in Swiss-Prot (35.20%), 17,372 in PFAM (38.14%), 17,372 in GO (38.14%), and 7,878 in KOG (17.29%) (Figures 2, 3 and Table 4).

Using a BLAST search compared to the NR database, matching these unigenes by species classification revealed that the number of hits between *P. fulvidraco* and *Ictalurus punctatus* were the highest (70.1%), followed by *Pygocentrus nattereri* (4.7%), *Astyanax mexicanus* (3.9%), *Cyprinus carpio* (1.7%), *Oncorhynchus mykiss* (1.6%), and other vertebrates (18.0%) (Figure 4).

Functional annotation of genes

GO is widely used to classify genes and gene products over species (36). To further study the biological importance of the unigenes, we made use of Blast2GO to determine the functional categories (25). According to the NR annotation from NCBI, 17,372 unigenes were classified into three major categories (cellular components, biological processes, and molecular functions) and 55 subcategories. In the biological process category, most unigenes were assigned to single-organism processes, metabolic process subcategories and cellular processes. Many unigenes were associated with the cell fraction and cell, in the cellular component category. In the molecular function category, most of the unigenes were found to participate in binding and catalytic activity (Figure 5).

The KOG is a database that can classify isogenous gene products. It is assumed that each KOG protein comes from an ancestor protein (37). To predict their possible functions and classify them by the KOG database, 7,878 unigenes were classified into 26 functional categories (Figure 6). Among these, the signal transduction mechanisms (T, 1,335) included the most unigenes, followed by general function prediction only (R, 1,282) and post-translational modification, protein turnover, and chaperones (O, 854). A number of unigenes (V, 59) were classified to the defense mechanisms category, which indicated these unigenes may participate in immunity protection of yellow catfish. The unigenes resembled those acquired from the *Megalobrama amblycephala* (38).

The KEGG is a bioinformatic database for the systematic analysis of gene functions (39). In this study, 11,300 unigenes in total were designated to 232 known pathways. The largest group was "PI3K-Akt signaling pathway", which contains 351

TABLE 2 The quality of raw and clean reads.

Sample	Raw Reads	Clean Reads	Clean Bases	Error(%)	Q20(%)	Q30(%)	GC Content(%)
PBS	54,703,956	53,492,522	8.02G	0.03	96.93	92.43	44.74
V. cholerae	48,686,580	47,733,280	7.16G	0.03	96.7	91.63	45.6

TABLE 3 Distribution of splicing length.

	Total nucleotide	Min length	Mean length	Median length	Max length	N50	N90
Transcripts	226,790,028	301	1679	1024	19,263	2854	677
unigenes	62,537,256	301	1373	727	19,263	1439	536

unigenes, followed by "Endocytosis" (330), "MAPK signaling pathway" (286), "Focal adhesion" (271), and "Rap1 signaling pathway" (257) (Table 5). Moreover, these 232 pathways were divided into five categories: environmental information processing, cellular processes, metabolism and organismal systems, and genetic information processing (Figure 7). Within the organismal systems, "endocrine system" (771) and "immune system" (785) were the two richest subcategories. In the metabolism category, the most common categories were "amino acid metabolism" (252), "lipid metabolism" (331) and "carbohydrate metabolism" (320). In the signal transduction category, the unigenes were mostly associated with environmental Information Processing (1686).
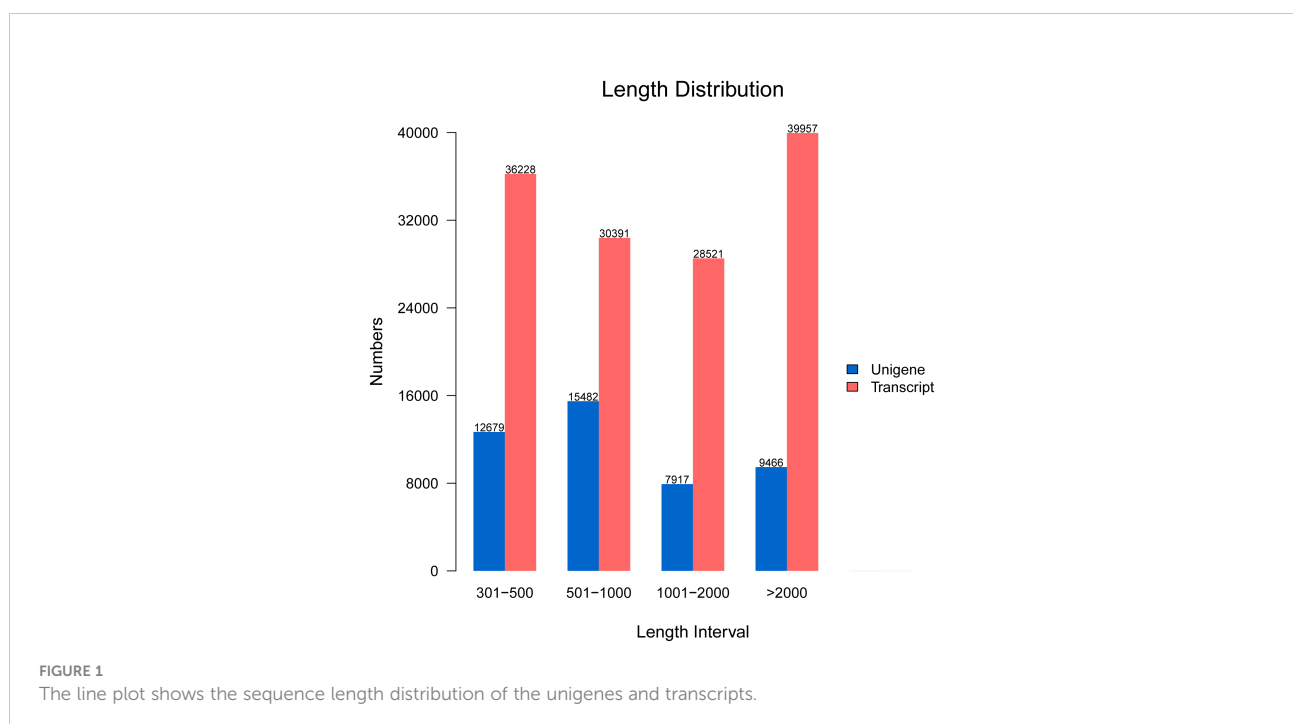
Identification of DEGs analysis

To recover the expression levels in the PBS- and *V. cholerae*-injected libraries, all unigenes were analyzed by RSEM software, and DEG-seq was applied to determine the DEGs when the Q-value < 0.005 and |log$_2$(fold change)|>1. A total of 674 differential expression genes were induced, of which 352 were significantly upregulated and 321 were significantly downregulated unigenes (Figure 8).

DEGs analysis

To further investigate the function of DEGs implicated in the immune response of *P. fulvidraco* challenged with *V. cholerae*, DEGs were compared with the KEGG database for pathway enrichment to understand the pathway, and 210 pathways in total were annotated. The top 20 of these divided pathways were shown in Table 6 and Figure 9. The largest quantities of DEGs appeared in the category "Ribosome", followed by "Endocytosis", and "Oxidative phosphorylation". Additionally, from 11 immune-related signal pathways, we identified 29 genes, including "Antigen processing and presentation" (9 DEGs), "Fc gamma R-mediated phagocytosis" (2 DEGs), "Leukocyte transendothelial migration" (10 DEGs), "TNF signaling pathway" (3 DEGs), "Toll-like receptor signaling pathway" (1 DEG), "Chemokine signaling pathway" (2 DEGs), "MAPK signaling pathway" (1 DEG), "NOD-like receptor

FIGURE 1
The line plot shows the sequence length distribution of the unigenes and transcripts.
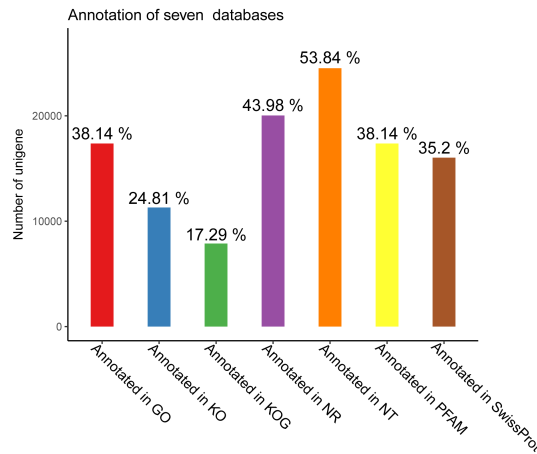
FIGURE 2
Annotated unigenes in seven databases.

signaling pathway" (2 DEGs), "Platelet activation" (2 DEGs), "Intestinal immune network for IgA production" (3 DEGs), and "NF-kappa B signaling pathway" (3 DEGs).

The validation of DEGs by qRT-PCR

Furthermore, to verify the differentially expressed genes, 10 genes were selected for qPT-PCR analysis challenged by *V. cholerae* for 6 h. The results showed that, compared with the control group, most immune related genes were upregulated at different points (Figure 10). The cadherin gene family plays a key role in target recognition and cell adhesion (40). Compared with the control group, cadherin-5 expression was significantly increased by more than double in the experimental group. In addition, cadherin is a transmembrane cell adhesion molecule conserved in metazoan organisms and plays an important role in histomorphogenesis and homeostasis (41). CC chemokines are a group of 28 chemokines with N-terminal CC domain, which play key roles in regulating leukocyte transport to injury, infection, or inflammation sites (42). The CC chemokine SCYA101 gene in *P. fulvidraco* was overexpressed by more than two-fold in response to *V. cholerae*. Moreover, calumenin (calu) is a well-conserved multi-EF-hand-containing Ca^{2+}-binding protein, which may provide a new target for bladder cancer and has multiple mechanisms, including TME remodeling, gene mutation, and ferroptosis (43). After injection of
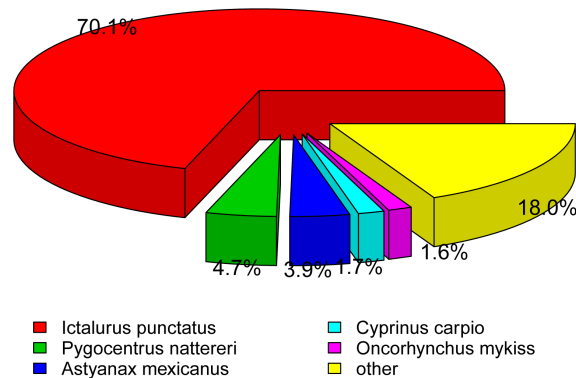

FIGURE 3
Map of species distribution in the NR database.

TABLE 4 Statistics of annotation.

	Number of genes	Percentage (%)
Annotated in NT	20034	43.98
Annotated in NR	24521	53.84
Annotated in KO	11300	24.81
Annotated in SwissProt	16032	35.2
Annotated in PFAM	17372	38.14
Annotated in GO	17372	38.14
Annotated in KOG	7878	17.29
Annotated in all Databases	5544	12.17
Annotated in at least one Database	29004	63.68
Total Unigenes	45544	100

V. cholerae, the expression level of calu was higher than that of the control group. Additionally, C-type lectins (CTLs) are calcium-dependent, carbohydrate-binding, pattern recognition receptors that play important roles in the immune system and primarily bind carbohydrate-based or other ligands that are involved in recognizing pathogens and cell adhesion (44–46). Compared with PBS injection, expression of CTLs was increased by over 5-fold. As a closely related class I cytokine, Interleukin (IL)- 13 plays important

roles in the T helper (Th)-2 immune response *via* heterodimeric receptors (47). The integrin family is included in an assortment of cell processes, including cell proliferation, separation, and migration, and in the pathogenesis of disease (48). Lysosomal membrane glycoprotein 1 (LAMP 1) is an integral membrane protein of the lysosome, which plays an important role in lysosomal biogenesis, autophagy, immune response, and cholesterol homeostasis (49). Mucin is synthesized and secreted
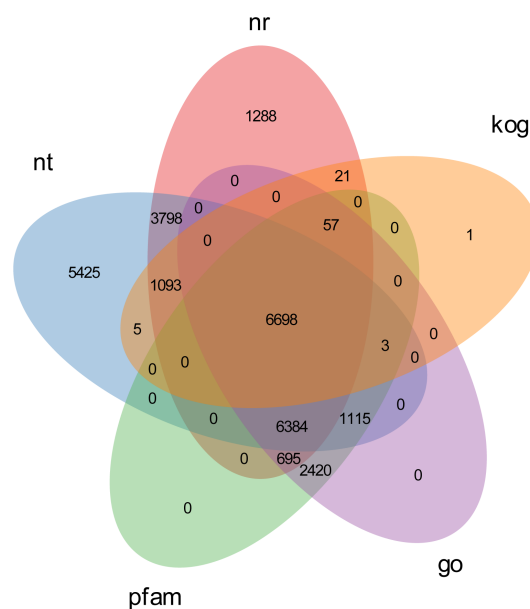
FIGURE 4
Venn diagram of overlap of the seven databases.

FIGURE 5

Gene ontology classifications of assembled unigenes. A total of 17,372 unigenes were categorized into three functional categories: biological process, cellular component, and molecular function.
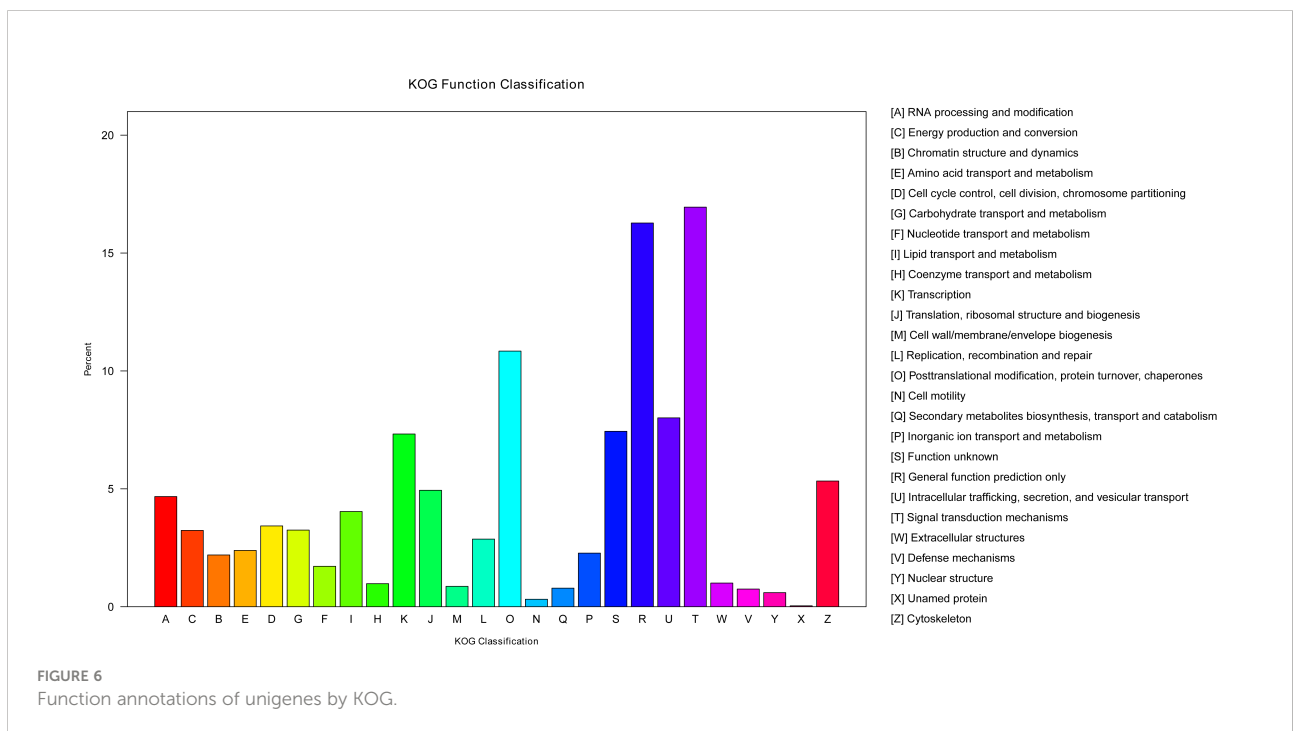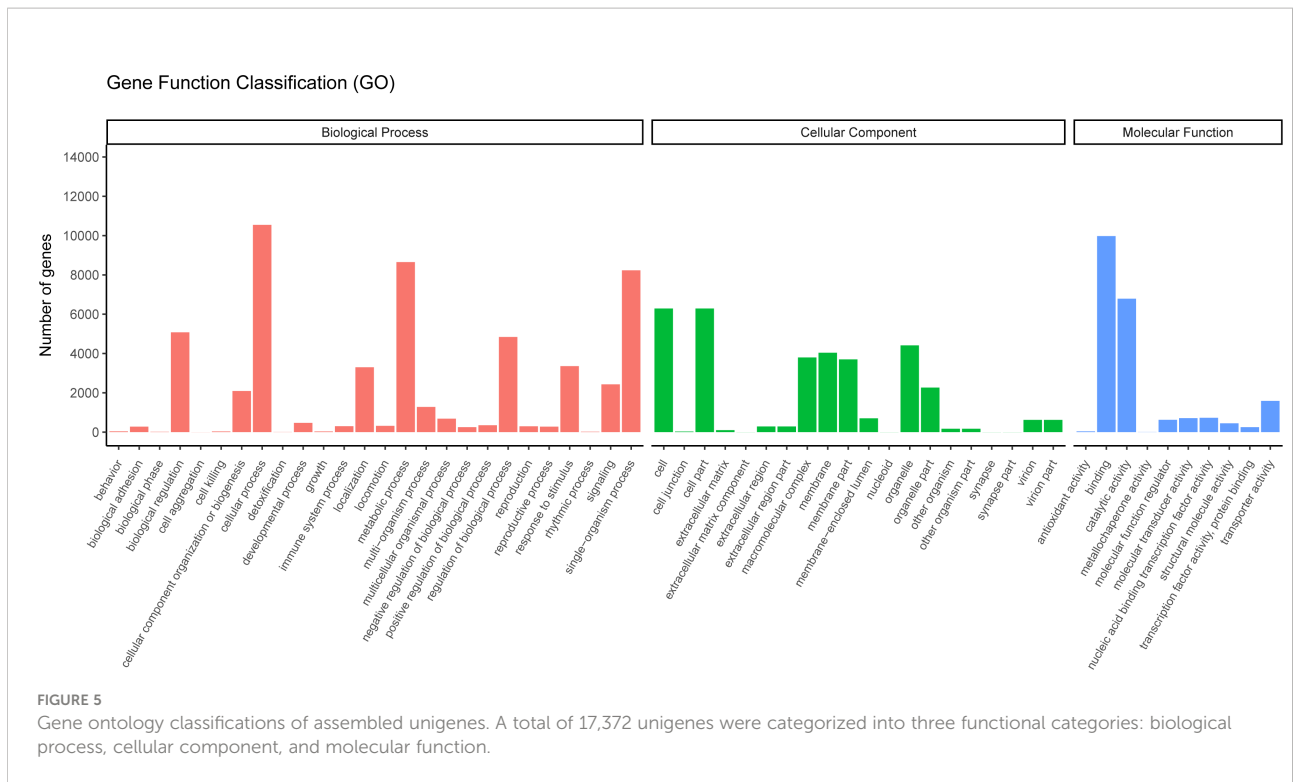

FIGURE 6

Function annotations of unigenes by KOG.

TABLE 5   KEGG annotation of assembled unigenes.

#	Pathway	Pathway ID	Number of unignes
1	PI3K-Akt signaling pathway	ko04151	351
2	Endocytosis	ko04144	330
3	MAPK signaling pathway	ko04010	286
4	Focal adhesion	ko04510	271
5	Rap1 signaling pathway	ko04015	257
6	Regulation of actin cytoskeleton	ko04810	251
7	Ras signaling pathway	ko04014	225
8	cAMP signaling pathway	ko04024	225
9	cGMP - PKG signaling pathway	ko04022	193
10	Chemokine signaling pathway	ko04062	187
11	Tight junction	ko04530	186
12	Axon guidance	ko04360	185
13	Oxytocin signaling pathway	ko04921	185
14	Calcium signaling pathway	ko04020	181
15	Thyroid hormone signaling pathway	ko04919	175
16	Protein processing in endoplasmic reticulum	ko04141	174
17	Purine metabolism	ko00230	174
18	Insulin signaling pathway	ko04910	173
19	Phagosome	ko04145	172
20	Hippo signaling pathway	ko04390	170
21	FoxO signaling pathway	ko04068	163
22	Platelet activation	ko04611	162
23	RNA transport	ko03013	160
24	Cytokine-cytokine receptor interaction	ko04060	154
25	Adrenergic signaling in cardiomyocytes	ko04261	153
26	Vascular smooth muscle contraction	ko04270	152
27	Ubiquitin mediated proteolysis	ko04120	150
28	Lysosome	ko04142	148
29	Neurotrophin signaling pathway	ko04722	147
30	AMPK signaling pathway	ko04152	146
31	Fc gamma R-mediated phagocytosis	ko04666	145
32	Signaling pathways regulating pluripotency of stem cells	ko04550	144
33	Wnt signaling pathway	ko04310	144
34	Sphingolipid signaling pathway	ko04071	141
35	Cell cycle	ko04110	140
36	Dopaminergic synapse	ko04728	139
37	Oocyte meiosis	ko04114	137

(Continued)

TABLE 5 Continued

#	Pathway	Pathway ID	Number of unignes
38	Spliceosome	ko03040	134
39	Osteoclast differentiation	ko04380	134
40	Oxidative phosphorylation	ko00190	132
41	Glucagon signaling pathway	ko04922	131
42	HIF-1 signaling pathway	ko04066	128
43	Leukocyte transendothelial migration	ko04670	126
44	Phosphatidylinositol signaling system	ko04070	124
45	Adherens junction	ko04520	123
46	Ribosome	ko03010	122
47	GnRH signaling pathway	ko04912	122
48	Carbon metabolism	ko01200	121
49	T cell receptor signaling pathway	ko04660	121
50	Neuroactive ligand-receptor interaction	ko04080	119
51	Estrogen signaling pathway	ko04915	118
52	Natural killer cell mediated cytotoxicity	ko04650	116
53	Jak-STAT signaling pathway	ko04630	115
54	Melanogenesis	ko04916	115
55	Cholinergic synapse	ko04725	113
56	TNF signaling pathway	ko04668	111
57	Circadian entrainment	ko04713	110
58	Glutamatergic synapse	ko04724	110
59	NF-kappa B signaling pathway	ko04064	107
60	Cell adhesion molecules (CAMs)	ko04514	107
61	Inflammatory mediator regulation of TRP channels	ko04750	104
62	B cell receptor signaling pathway	ko04662	103
63	ErbB signaling pathway	ko04012	101

by epithelial goblet cells, and is a key component of the innate immune system and plays an important part within the digestive system (50). The natterin protein family was first found in the venom of thalassophryne nattereri, a fish with medical significance. In the past decade, natterin-like genes have been found in various organisms, including genes that perform immune related functions (51). In conclusion, these immune genes may be related to the immune defense of *P. fulvidraco* after bacterial infection.

Conclusion

P. fulvidraco is a famous fresh-water fish with enormous economic value in eastern China. Raising a large number of *P.*

fulvidraco leads to the outbreak of various diseases and thus, economic losses. In this study, the transcriptomic characteristics following *V. cholerae* injection in the liver of *P. fulvidraco* were analyzed in detail. We identified a great deal of genes and pathways involved in the immunization to *V. cholerae* in *P. fulvidraco*. A total of 674 DEGs were identified, including 321 downregulated genes and 352 upregulated genes, some of which are related to "Antigen processing and presentation", "Fc gamma R-mediated phagocytosis", "Toll-like receptor signaling pathway" and other signaling pathways. These results were obtained for the first time in this work. In conclusion, this study may provide an opportunity to explore the immune defense mechanism of *P. fulvidraco* against bacterial attack.
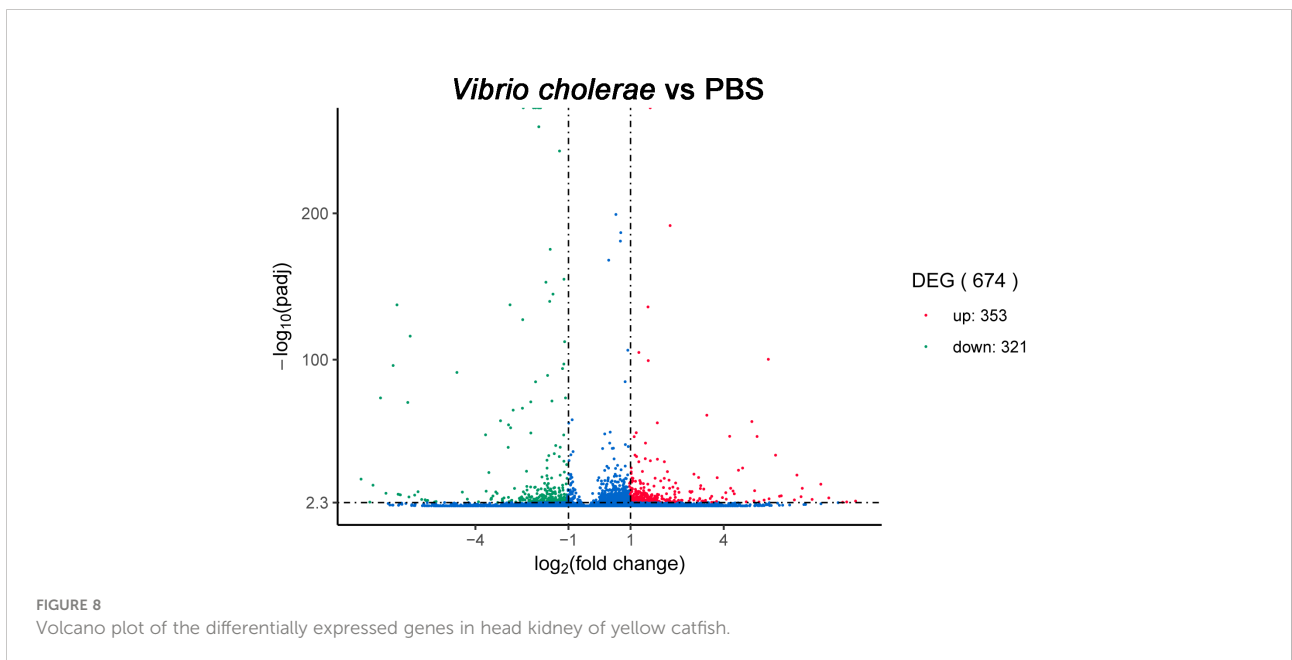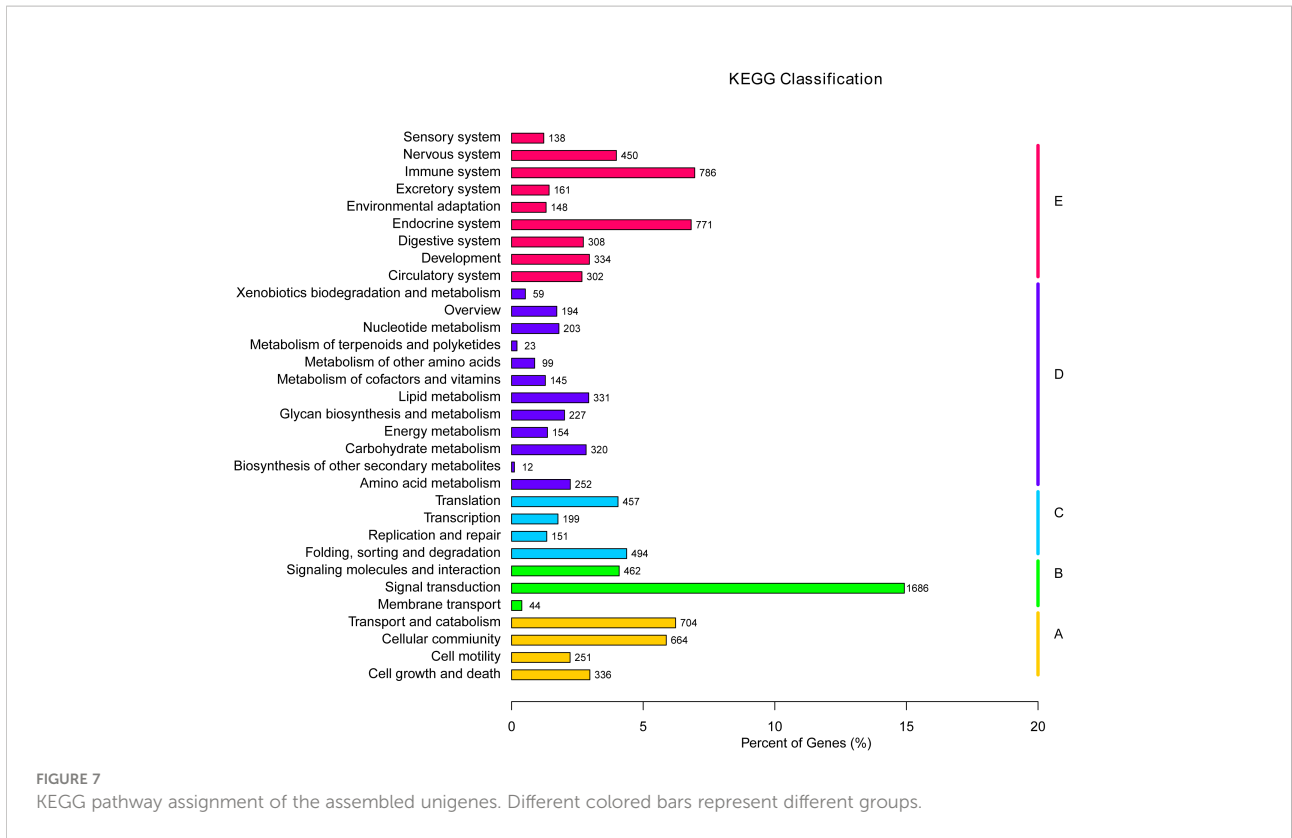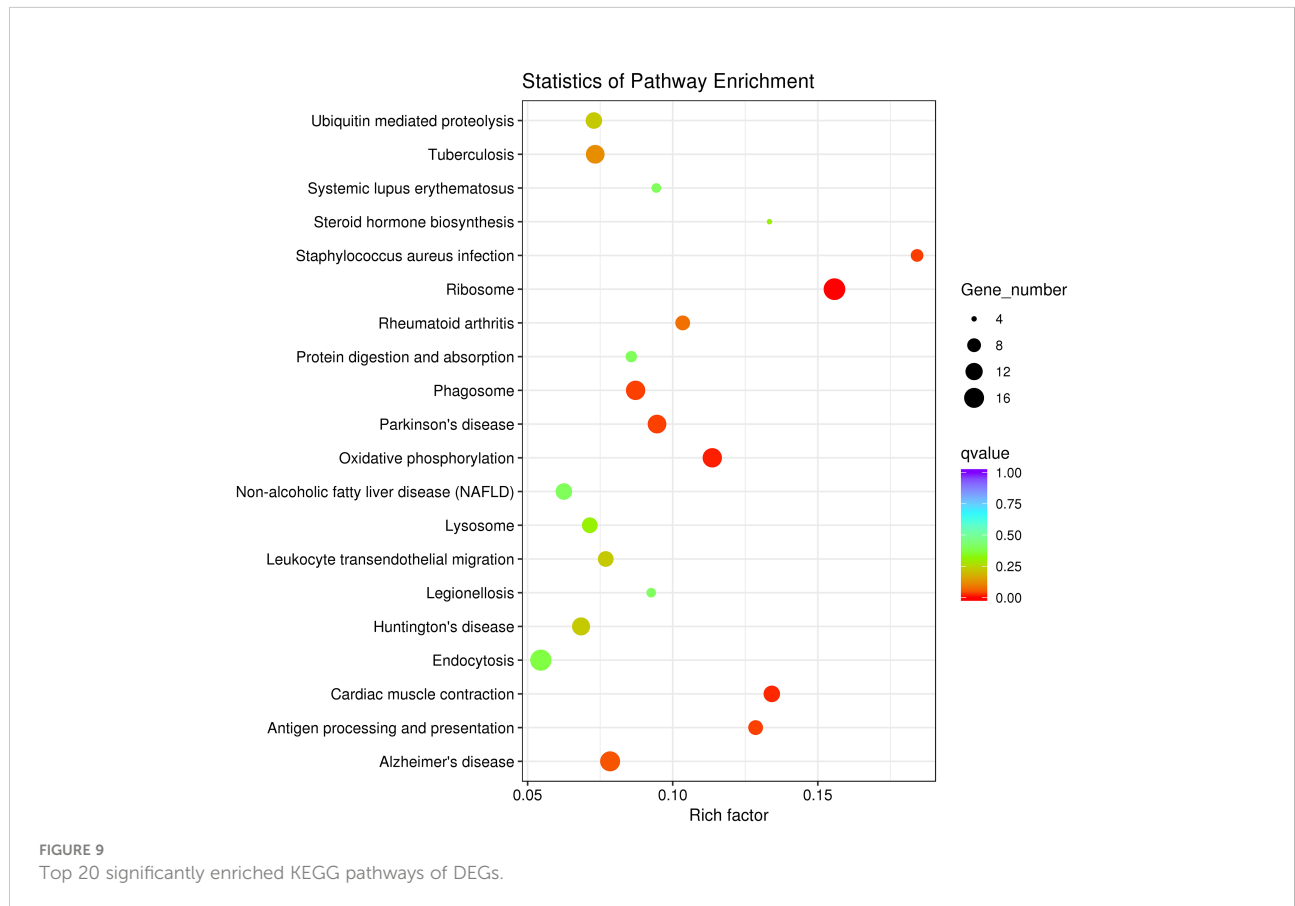
FIGURE 7
KEGG pathway assignment of the assembled unigenes. Different colored bars represent different groups.

FIGURE 8
Volcano plot of the differentially expressed genes in head kidney of yellow catfish.

TABLE 6 KEGG annotation of assembled unigenes.

pathway	ID	DEGs number
Antigen processing and presentation	ko04612	9
Fc gamma R-mediated phagocytosis	ko04666	2
Leukocyte transendothelial migration	ko04670	10
TNF signaling pathway	ko04668	3
Toll-like receptor signaling pathway	ko04620	1
Chemokine signaling pathway	ko04062	2
MAPK signaling pathway	ko04010	9
NOD-like receptor signaling pathway	ko04621	2
Lysosome	ko04142	10
Intestinal immune network for IgA production	ko04672	3
NF-kappa B signaling pathway	ko04064	3

FIGURE 9
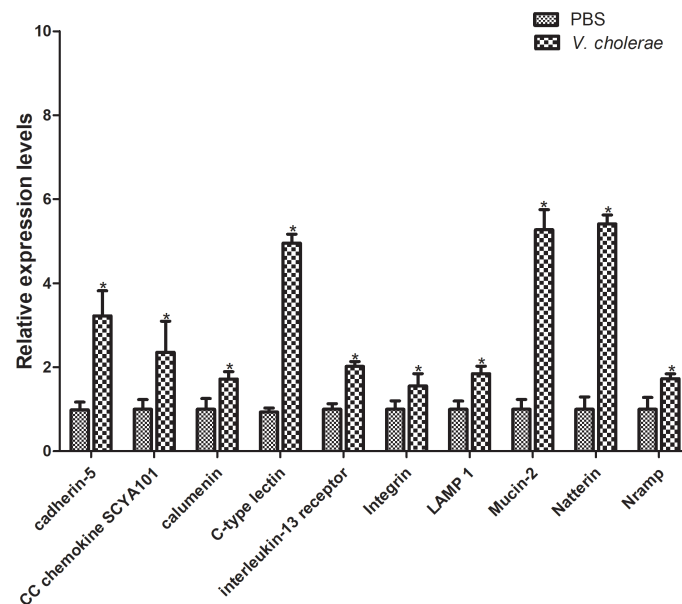Top 20 significantly enriched KEGG pathways of DEGs.

FIGURE 10
Validation of DEGs by qRT-PCR. The relative gene expression levels of 10 selected DEGs were examined. The β-actin gene was used as an internal standard. The means + SEM of three independent samples are shown (means $\pm$ SE, n = 3). Differences between treated and control samples were tested by one-way analysis of variance (ANOVA) followed by the Duncan's new multiple range test. The P values are shown as $*P < 0.05$.

Data availability statement

The datasets presented in this study can be found in online repositories. The names of the repository/repositories and accession number(s) can be found below: https://www.ncbi.nlm.nih.gov/genbank/, PRJNA902142.

Author contributions

The authors' responsibilities were as follows: S-HJ and Q-NL: Analyzed data, Wrote the manuscript. L-XW, Y-TC, H-BZ, and R-TM: Analyzed data and conducted experiments. D-ZZ: Resources. Q-NL: Funding acquisition. B-PT and L-SD: Experiment design and manuscript review and editing, Resources. All authors contributed to the article and approved the submitted version.

Funding

Conflict of interest

The authors declare that the research was conducted in the absence of any commercial or financial relationships that could be construed as a potential conflict of interest.

Publisher's note

All claims expressed in this article are solely those of the authors and do not necessarily represent those of their affiliated organizations, or those of the publisher, the editors and the reviewers. Any product that may be evaluated in this article, or claim that may be made by its manufacturer, is not guaranteed or endorsed by the publisher.

References

1. Yang RB, Xie CX, Fan QX, Gao C, Fang LB. Ontogeny of the digestive tract in yellow catfish *Pelteobagrus fulvidraco* larvae. *Aquaculture* (2010) 302(1):112–23. doi: 10.1016/j.aquaculture.2010.02.020

2. Gong G, Dan C, Xiao S, Guo W, Huang P, Xiong Y, et al. Chromosomal-level assembly of yellow catfish genome using third-generation DNA sequencing and Hi-c analysis. *Gigascience* (2018) 7(11):giy120. doi: 10.1093/gigascience/giy120

3. Hu YH, Zhou X, Jiang XX, Zhang GR, Shi ZC, Ji W, et al. Molecular characterization, expression analysis and function identification of Pf_TNF-α and its two receptors Pf_TNFR1 and Pf_TNFR2 in yellow catfish (Pelteobagrus fulvidraco). *Int J Biol Macromol* (2021) 185:176–93. doi: 10.1016/j.ijbiomac.2021.06.090

4. Zhao H, Wang G, Wang H, Mo W, Huang Y, Cao J, et al. Effects of dietary sodium butyrate on growth, digestive enzymes, body composition and nutrient retention-related gene expression of juvenile yellow catfish (*Pelteobagrus fulvidraco*). *Anim Nutr* (2021) 7(2):539–47. doi: 10.1016/j.aninu.2020.12.007

5. Liu Y, Wu PD, Zhang DZ, Zhang HB, Tang BP, Liu QN, et al. Mitochondrial genome of the yellow catfish *Pelteobagrus fulvidraco* and insights into bagridae phylogenetics. *Genomics* (2019) 111(6):1258–65. doi: 10.1016/j.ygeno.2018.08.005

6. Lu SF, Zhao N, Zhao A, He RG. Effect of soybean phospholipid supplementation in formulated microdiets and live food on foregut and liver histological changes of *Pelteobagrus fulvidraco* larvae. *Aquaculture* (2008) 278:119–27. doi: 10.1016/j.aquaculture.2007.12.007

7. Liu HQ, Guan B, Xu J, Hou CC, Tian H, Chen HX. Genetic manipulation of sex ratio for the large-scale breeding of YY super-male and XY all-male yellow catfish (*Pelteobagrus fulvidraco* (Richardson)). *Mar Biotechnol* (2013) 15:321–8. doi: 10.1007/s10126-012-9487-7

8. Zheng JL, Luo Z, Zhu QL, Tan XY, Chen QL, Sun LD, et al. Molecular cloning and expression pattern of 11 genes involved in lipid metabolism in yellow catfish pelteobagrus fulvidraco. *Gene* (2013) 531(1):53–63. doi: 10.1016/j.gene.2013.08.028

9. Zhou X, Zhang GR, Ji W, Shi ZC, Ma XF, Luo ZL, et al. The dynamic immune response of yellow catfish (*Pelteobagrus fulvidraco*) infected with edwardsiella ictaluri presenting the inflammation process. *Front Immunol* (2021) 12:625928. doi: 10.3389/fimmu.2021.625928

10. Chen K, Zhao F, Ouyang G, Shi Z, Ma L, Wang B, et al. Molecular characterization and expression analysis of Tf_TLR4 and Tf_TRIL in yellow catfish *Tachysurus fulvidraco* responding to *Edwardsiella ictaluri* challenge. *Int J Biol Macromol* (2021) 167:746–55. doi: 10.1016/j.ijbiomac.2020.11.196

11. Wang S, Li X, Zhang M, Jiang H, Wang R, Qian Y, et al. Ammonia stress disrupts intestinal microbial community and amino acid metabolism of juvenile yellow catfish (*Pelteobagrus fulvidraco*). *Ecotoxicol Environ Saf* (2021) 227:112932. doi: 10.1016/j.ecoenv.2021.112932

12. Das B, Pazhani GP, Sarkar A, Mukhopadhyay AK, Nair GB, Ramamurthy T. Molecular evolution and functional divergence of vibrio cholerae. *Curr Opin Infect Dis* (2016) 29(5):520–7. doi: 10.1097/QCO.0000000000000306

13. Dillies MA, Rau A, Aubert J, Hennequet-Antier C, Jeanmougin M, Servant N, et al. A comprehensive evaluation of normalization methods for illumina high-throughput RNA sequencing data analysis. *Brief Bioinform* (2013) 14(6):671–83. doi: 10.1093/bib/bbs046

14. Mortazavi A, Williams BA, McCue K, Schaeffer L, Wold B. Mapping and quantifying mammalian transcriptomes by RNA-seq. *Nat Methods* (2008) 5 (7):621–8. doi: 10.1038/nmeth.1226

15. Jiang Z, Zhou X, Li R, Michal JJ, Zhang S, Dodson MV, et al. Whole transcriptome analysis with sequencing: methods, challenges and potential solutions. *Cell Mol Life Sci* (2015) 72(18):3425–39. doi: 10.1007/s00018-015-1934-y

16. Zhou Y, Zhu L, Sun Y, Zhang H, Wang J, Qin W, et al. Localization of RNA pol II CTD (S5) and transcriptome analysis of testis in diploid and tetraploid hybrids of red crucian carp (♀) × common carp (♂). *Front Genet* (2021) 12:717871. doi: 10.3389/fgene.2021.717871

17. Roh H, Kim N, Lee Y, Park J, Kim BS, Lee MK, et al. Dual-organ transcriptomic analysis of rainbow trout infected with ichthyophthirius multifiliis through Co-expression and machine learning. *Front Immunol* (2021) 12:677730. doi: 10.3389/fimmu.2021.677730

18. Lin G, Gao D, Lu J, Sun X. Transcriptome profiling reveals the sexual dimorphism of gene expression patterns during gonad differentiation in the half-smooth tongue sole (Cynoglossus semilaevis). *Mar Biotechnol (NY)* (2021) 23 (1):18–30. doi: 10.1007/s10126-020-09996-x

19. Wang Z, Jia Y, Huang X, Zhu D, Liu H, Wang W. Transcriptome profiling towards understanding of the morphogenesis in the scale development of blunt snout bream (*Megalobrama amblycephala*). *Genomics* (2021) 113(3):983–91. doi: 10.1016/j.ygeno.2020.12.043

20. Zheng Y, Wu W, Hu G, Qiu L, Chen J. Transcriptome analysis of juvenile tilapia (*Oreochromis niloticus*) blood, fed with different concentrations of resveratrol. *Front Physiol* (2020) 11:600730. doi: 10.3389/fphys.2020.600730

21. Qi Z, Wu P, Zhang Q, Wei Y, Wang Z, Qiu M, et al. Transcriptome analysis of soiny mullet (*Liza haematocheila*) spleen in response to streptococcus dysgalactiae. *Fish Shellfish Immunol* (2016) 49:194–204. doi: 10.1016/j.fsi.2015.12.029

22. Chu Q, Song W, Cui J, Xu T. Genome-guided transcriptome analysis of miiuy croaker provides insights into pattern recognition receptors and cytokines in response to vibrio anguillarum. *Dev Comp Immunol* (2017) 73:72–8. doi: 10.1016/j.dci.2017.03.009

23. Geven EJW, Klaren PHM. The teleost head kidney: Integrating thyroid and immune signalling. *Dev Comp Immunol* (2017) 66:73–83. doi: 10.1016/j.dci.2016.06.025

24. Grabherr MG, Haas BJ, Yassour M, Levin JZ, Thompson DA, Amit I, et al. Full-length transcriptome assembly from RNA-seq data without a reference genome. *Nat Biotechnol* (2011) 29(7):644–52. doi: 10.1038/nbt.1883

25. Conesa A, Götz S, García-Gómez JM, Terol J, Talón M, Robles M. Blast2GO: A universal tool for annotation, visualization and analysis in functional genomics research. *Bioinformatics* (2005) 21(18):3674–6. doi: 10.1093/bioinformatics/bti610

26. Ye J, Zhang Y, Cui H, Liu J, Wu Y, Cheng Y, et al. WEGO 2.0: a web tool for analyzing and plotting GO annotations, 2018 update. *Nucleic Acids Res* (2018) 46 (W1):W71–5. doi: 10.1093/nar/gky400

27. Kanehisa M, Furumichi M, Tanabe M, Sato Y, Morishima K. KEGG: new perspectives on genomes, pathways, diseases and drugs. *Nucleic Acids Res* (2017) 45 (D1):D353–61. doi: 10.1093/nar/gkw1092

28. Trapnell C, Williams BA, Pertea G, Mortazavi A, Kwan G, van Baren MJ, et al. Transcript assembly and quantification by RNA-seq reveals unannotated transcripts and isoform switching during cell differentiation. *Nat Biotechnol* (2010) 28(5):511–5. doi: 10.1038/nbt.1621

29. Li B, Dewey CN. RSEM: accurate transcript quantification from RNA-seq data with or without a reference genome. *BMC Bioinf* (2011) 12:323. doi: 10.1186/1471-2105-12-323

30. Robinson MD, McCarthy DJ, Smyth GK. edgeR: a bioconductor package for differential expression analysis of digital gene expression data. *Bioinformatics* (2010) 26(1):139–40. doi: 10.1093/bioinformatics/btp616

31. Wang L, Feng Z, Wang X, Wang X, Zhang X. DEGseq: an r package for identifying differentially expressed genes from RNA-seq data. *Bioinformatics* (2010) 26(1):136–8. doi: 10.1093/bioinformatics/btp612

32. Young MD, Wakefield MJ, Smyth GK, Oshlack A. Gene ontology analysis for RNA-seq: accounting for selection bias. *Genome Biol* (2010) 11(2):R14. doi: 10.1186/gb-2010-11-2-r14

33. Mao X, Cai T, Olyarchuk JG, Wei L. Automated genome annotation and pathway identification using the KEGG orthology (KO) as a controlled vocabulary. *Bioinformatics* (2005) 21(19):3787–93. doi: 10.1093/bioinformatics/bti430

34. Livak KJ, Schmittgen TD. Analysis of relative gene expression data using real-time quantitative PCR and the 2(-delta delta C(T)) method. *Methods* (2001) 25 (4):402–8. doi: 10.1006/meth.2001.1262

35. Chalifa-Caspi V. RNA-Seq in nonmodel organisms. *Methods Mol Biol* (2021) 2243:143–67. doi: 10.1007/978-1-0716-1103-6_8

36. Gabaldón T, Koonin EV. Functional and evolutionary implications of gene orthology. *Nat Rev Genet* (2013) 14(5):360–6. doi: 10.1038/nrg3456

37. Jensen LJ, Julien P, Kuhn M, von Mering C, Muller J, Doerks T, et al. eggNOG: automated construction and annotation of orthologous groups of genes. *Nucleic Acids Res* (2008) 36(Database issue):D250–4. doi: 10.1093/nar/gkm796

38. Tran NT, Gao ZX, Zhao HH, Yi SK, Chen BX, Zhao YH, et al. Transcriptome analysis and microsatellite discovery in the blunt snout bream (Megalobrama amblycephala) after challenge with aeromonas hydrophila. *Fish Shellfish Immunol* (2015) 45(1):72–82. doi: 10.1016/j.fsi.2015.01.034

39. Kanehisa M, Furumichi M, Sato Y, Ishiguro-Watanabe M, Tanabe M. KEGG: integrating viruses and cellular organisms. *Nucleic Acids Res* (2021) 49 (D1):D545–51. doi: 10.1093/nar/gkaa970

40. Sadeqzadeh E, de Bock CE, Thorne RF. Sleeping giants: emerging roles for the fat cadherins in health and disease. *Med Res Rev* (2014) 34(1):190–221. doi: 10.1002/med.21286

41. Tiwari P, Mrigwani A, Kaur H, Kaila P, Kumar R, Guptasarma P. Structural-mechanical and biochemical functions of classical cadherins at cellular junctions: A review and some hypotheses. *Adv Exp Med Biol* (2018) 1112:107–38. doi: 10.1007/978-981-13-3065-0_9

42. Palomino DC, Marti LC. Chemokines and immunity. *Einstein (Sao Paulo)* (2015) 13(3):469–73. doi: 10.1590/S1679-45082015RB3438

43. Du Y, Miao W, Jiang X, Cao J, Wang B, Wang Y, et al. The epithelial to mesenchymal transition related gene calumenin is an adverse prognostic factor of bladder cancer correlated with tumor microenvironment remodeling, gene mutation, and ferroptosis. *Front Oncol* (2021) 11:683951. doi: 10.3389/fonc.2021.683951

44. Ng TB, Fai Cheung RC, Wing Ng CC, Fang EF, Wong JH. A review of fish lectins. *Curr Protein Pept Sci* (2015) 16(4):337–51. doi: 10.2174/138920371604150429160850

45. Mu L, Yin X, Wu H, Han K, Guo Z, Ye J. MAp34 regulates the non-specific cell immunity of Monocytes/Macrophages and inhibits the lectin pathway of complement activation in a teleost fish. *Front Immunol* (2020) 11:1706. doi: 10.3389/fimmu.2020.01706

46. Petit J, Bailey EC, Wheeler RT, de Oliveira CAF, Forlenza M, Wiegertjes GF. Studies into β-glucan recognition in fish suggests a key role for the c-type lectin pathway. *Front Immunol* (2019) 10:280. doi: 10.3389/fimmu.2019.00280

47. Sequeida A, Maisey K, Imarai M. Interleukin 4/13 receptors: An overview of genes, expression and functional role in teleost fish. *Cytokine Growth Factor Rev* (2017) 38:66–72. doi: 10.1016/j.cytogfr.2017.09.004

48. Sun G, Guillon E, Holley SA. Integrin intra-heterodimer affinity inversely correlates with integrin activatability. *Cell Rep* (2021) 35(10):109230. doi: 10.1016/j.celrep.2021.109230

49. Alessandrini F, Pezzè L, Ciribilli Y. LAMPs: Shedding light on cancer biology. *Semin Oncol* (2017) 44(4):239–53. doi: 10.1053/j.seminoncol.2017.10.013

50. Gao X, Cao Q, Cheng Y, Zhao D, Wang Z, Yang H, et al. Chronic stress promotes colitis by disturbing the gut microbiota and triggering immune system response. *Proc Natl Acad Sci USA* (2018) 115(13):E2960–9. doi: 10.1073/pnas.1720696115

51. Lima C, Disner GR, Falcão MAP, Seni-Silva AC, Maleski ALA, Souza MM, et al. The natterin proteins diversity: A review on phylogeny, structure, and immune function. *Toxins (Basel)* (2021) 13(8):538. doi: 10.3390/toxins13080538